Supporting Information

Axial Coordination-Assisted Interwoven Isomerism in 3D Hydrogen-Bonded Organic Frameworks for Efficient Natural Gas Purification

Hyunjun Park[1‡], Kwang Hyun Oh[2‡], Jae Hwa Lee[3‡], Younghun Kim[1], Jeong Heon Lee[1], Hoi Ri Moon[4], Youn-Sang Bae[2]*, and Woo-Dong Jang[1]**

[1]Department of Chemistry, Yonsei University, 50 Yonsei-ro, Seodaemun-gu, Seoul 03722, Republic of Korea

[2]Department of Chemical and Biomolecular Engineering, Yonsei University, 50 Yonsei-ro, Seodaemun-gu, Seoul 03722, Republic of Korea

[3]Department of Chemistry, Ulsan National Institute of Science and Technology (UNIST), 50, UNIST-gil, Ulsan 44919, Republic of Korea

[4]Department of Chemistry and Nanoscience, Ewha Womans University, Seoul 03760, Republic of Korea

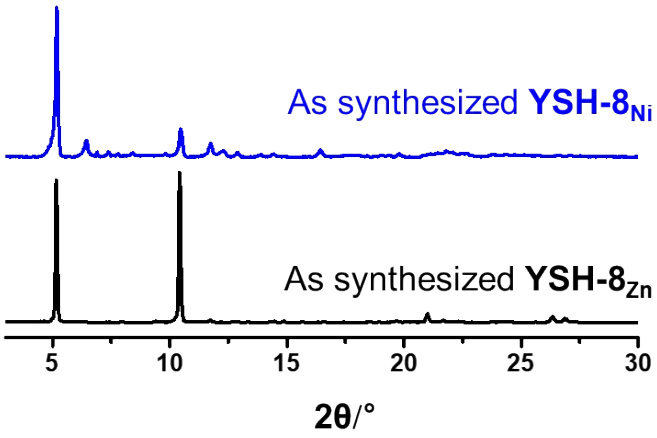

Figure S1. PXRD pattern of a) **YSH-8$_{Zn}$** and b) **YSH-8$_{Ni}$**.

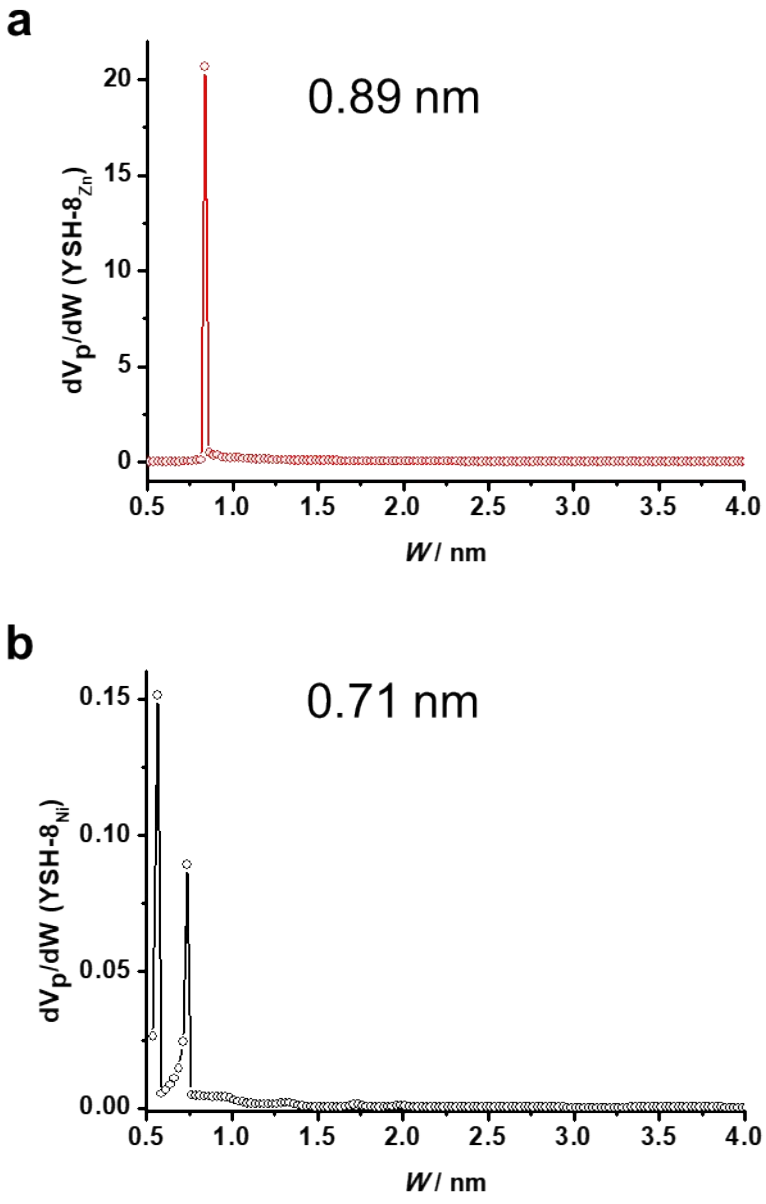

Figure S2. Pore size distribution of a) **YSH-8$_{Zn/Hx}$***, b) **YSH-8$_{Ni}$***.

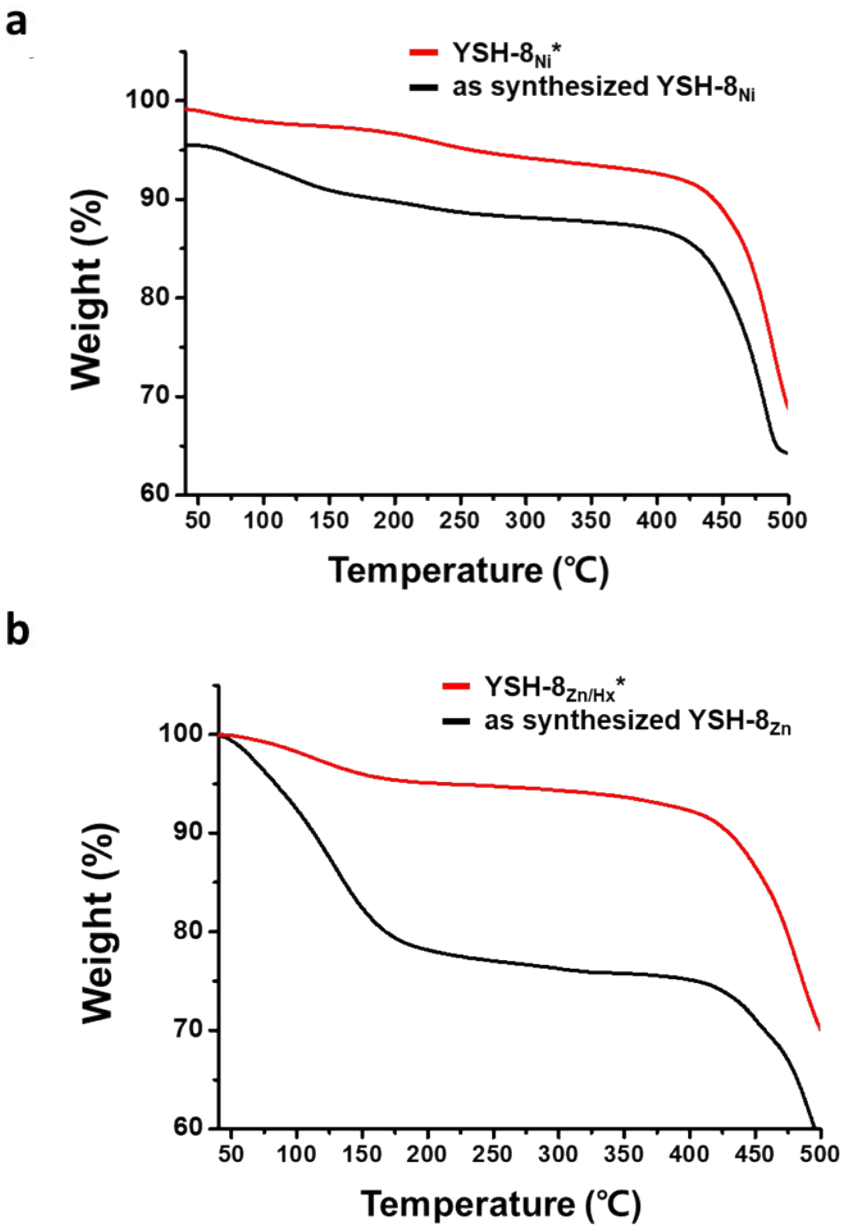

Figure S3. TGA curve of **a) YSH-8$_{Ni}$** and **b) YSH-8$_{Zn}$**.

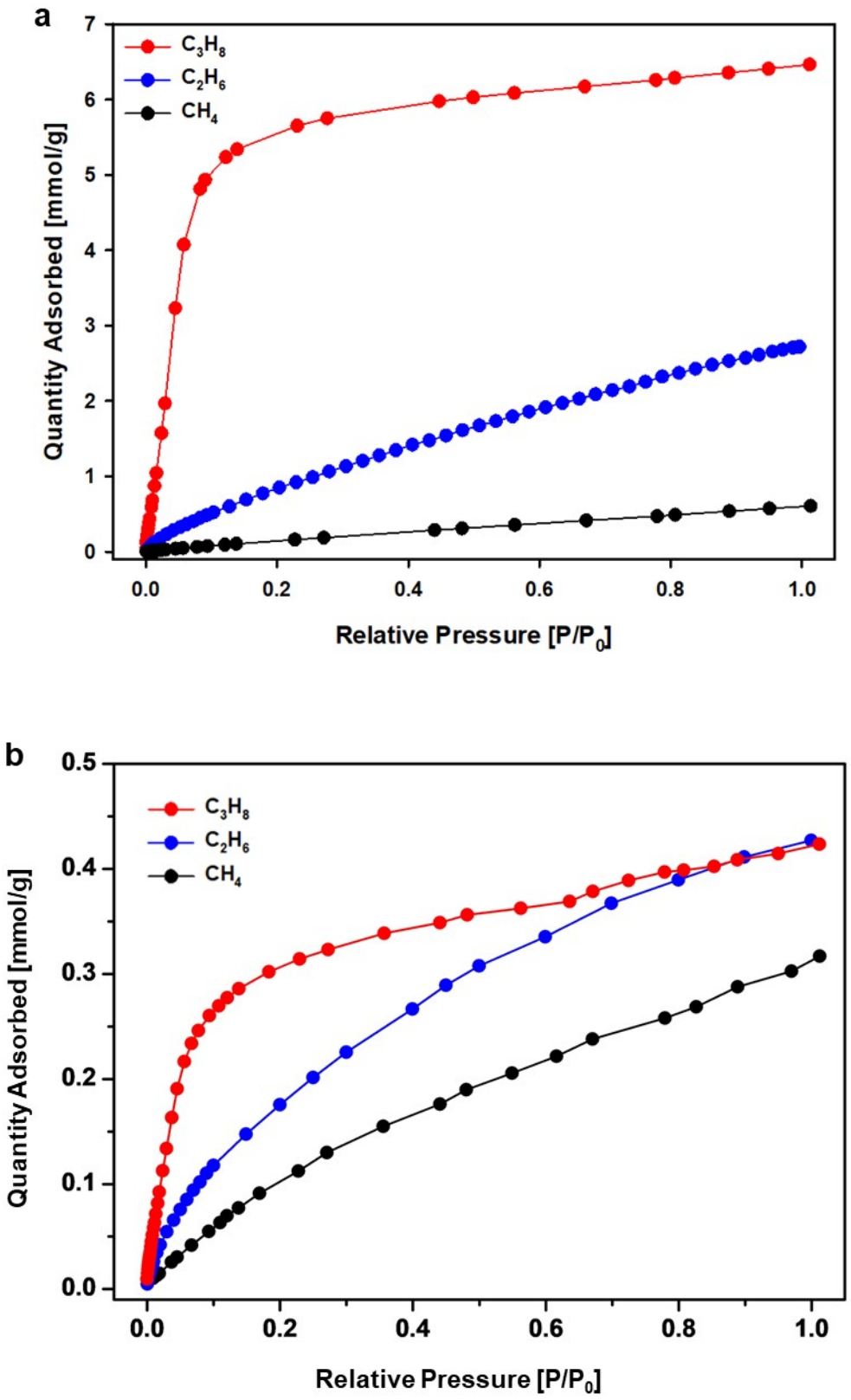

Figure S4. Single gas absorption isotherm of C_3H_8, C_2H_6 and CH_4 at 273 K of a) **YSH-8**$_{Zn/Hx}$* and b) **YSH-8**$_{Ni}$*.

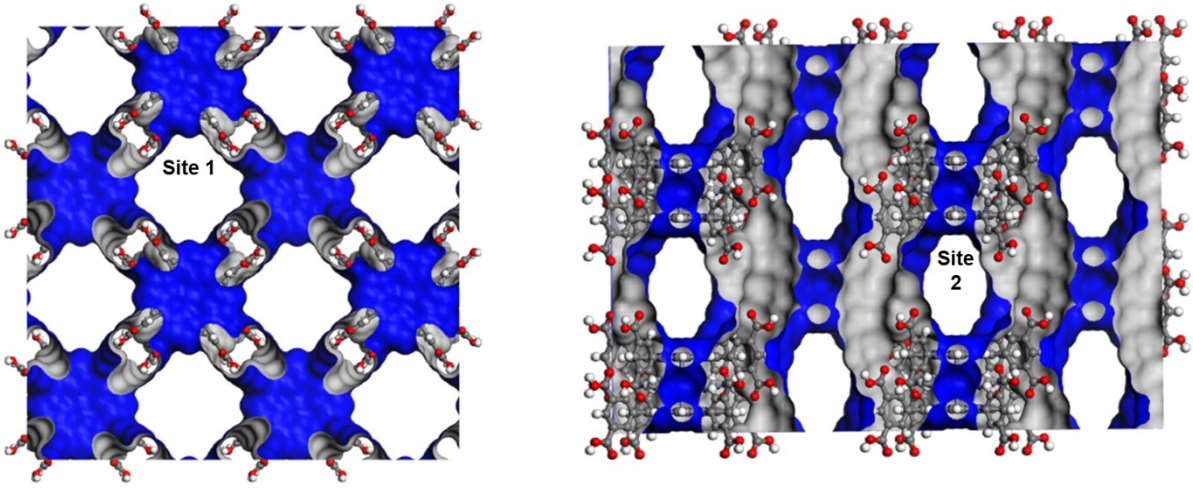

Figure S5. Adsorption site of C_3H_8 and C_2H_6 in **YSH-8$_{Zn/Hx}$**.

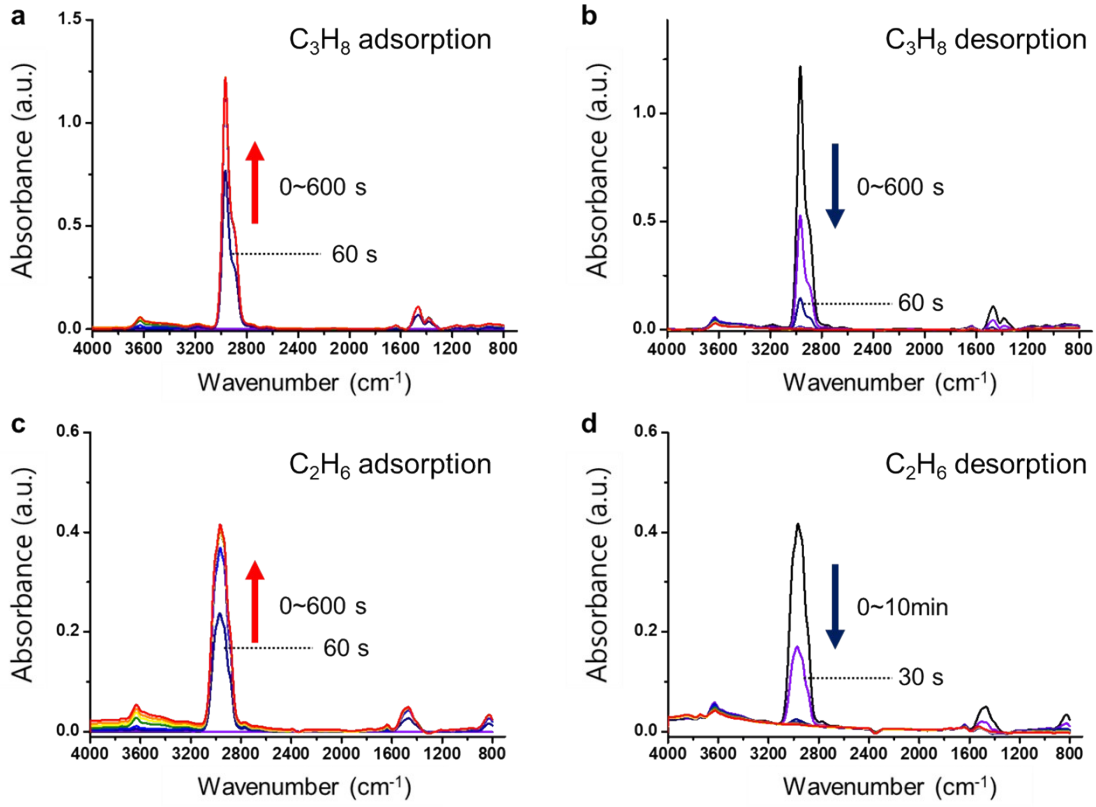

Figure S6. In-situ DRIFT spectra of **YSH-8$_{Zn/Hx}$*** a) C_3H_8 adsorption, b) C_3H_8 desorption; c) C_2H_6 adsorption and d) C_2H_6 desorption.

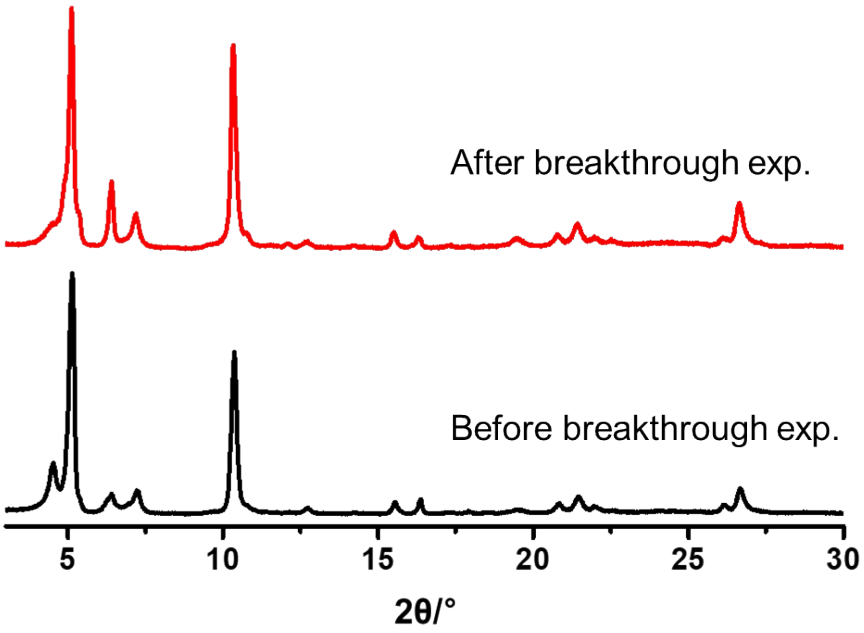

Figure S7. PXRD pattern of **YSH-8$_{Zn}$*** after breakthrough experiment.

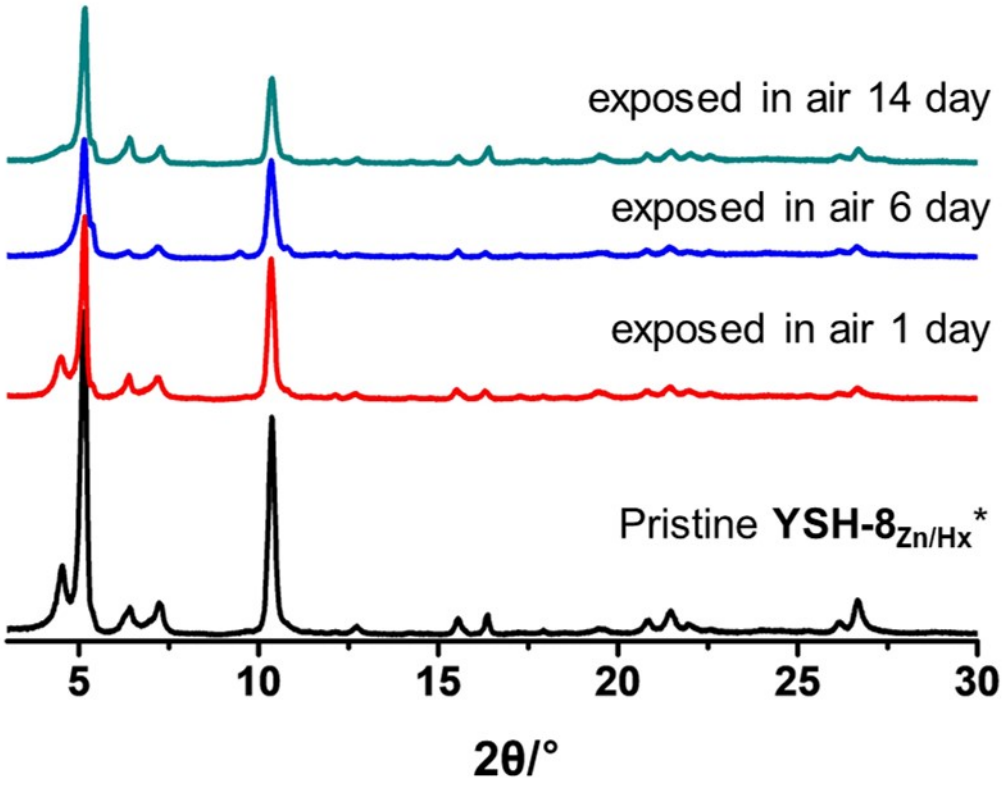

Figure S8. PXRD pattern of **YSH-8$_{Zn/Hx}$*** after exposure in air.

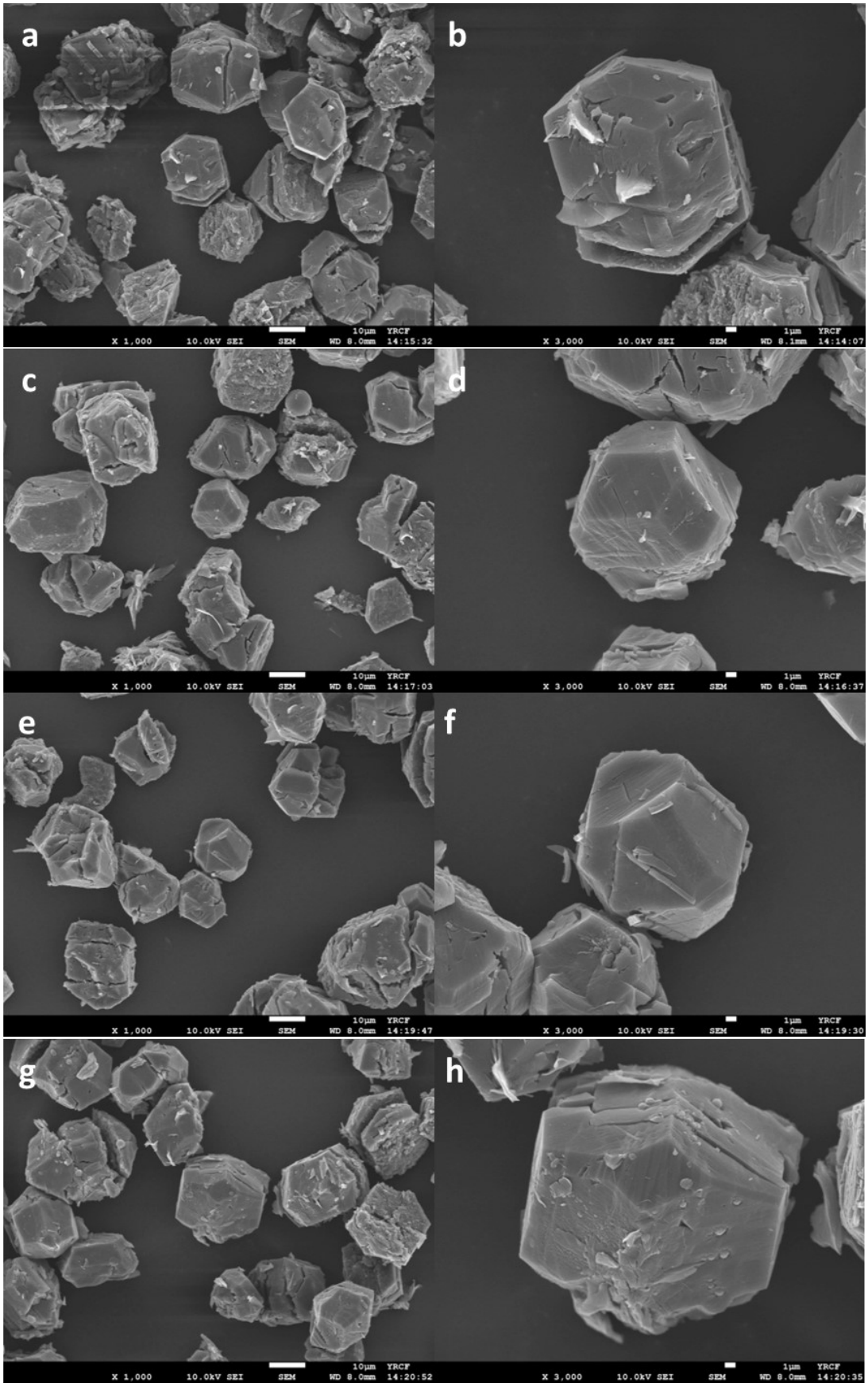

Figure S9. SEM images of **YSH-8$_{Zn/Hx}$*** a) and b) pristine; c) and d) after C_3H_8 adsorption; e) and f) after C_2H_6 adsorption; g) and h) after CH_4 adsorption.

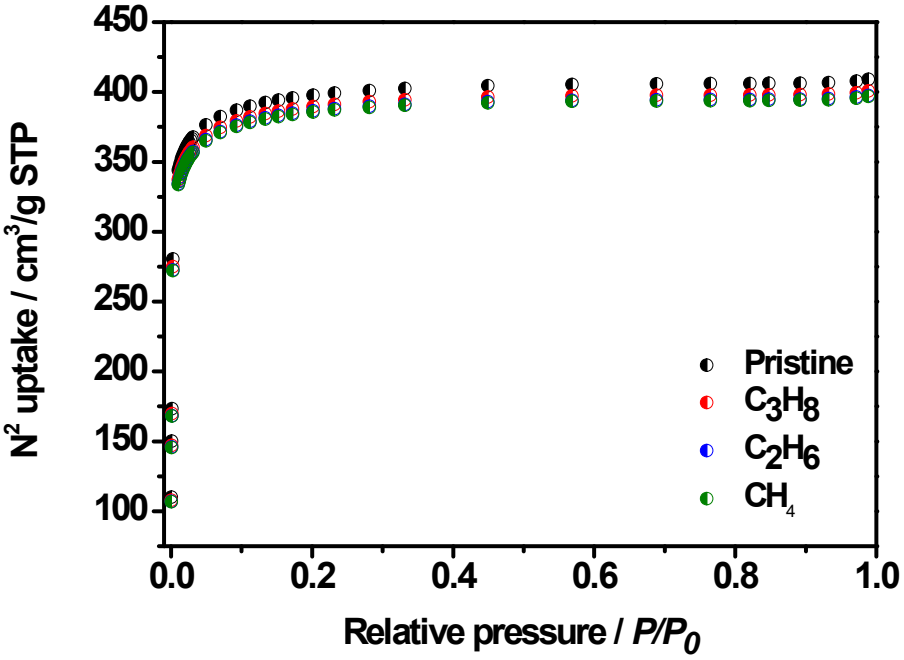

Figure S10. Comparison of 77K N_2 Isotherm of **YSH-8$_{Zn/Hx}$*** after C_3H_8, C_2H_6, and CH_4 adsorption.

Table S1. Comparison with benchmark adsorbents.

Material	BET surface area (m^2/g)	Gas uptake at 298 K (mmol/g)			IAST (298 K/ gas ratio 50:50)			Ref.
		C_3H_8	C_2H_6	CH_4	C_3H_8/C_2H_6	C_3H_8/CH_4	C_2H_6/CH_4	
YSH-8$_{Zn/Hx}$*	1665	6.46	2.06	0.239	36.9	492	22.2	This work
MOF 1	1125	3.56	4.55	0.68	10.9	638.9	61.0	[1]
ZUL-C2	417	2.52	2.82	-	-	632	91	[2]
UPC-99	886	4.85	2.72	0.44	4.9	426.8	-	[3]
BSF-1	535	1.94	1.57	0.47	-	353	23	[4]
UPC-100-IN	1677.7	5.30	3.15	0.52	-	186.4	-	[5]
JLU-Liu45	971	3.79	3.78	0.69		42.7	20.1	[6]
UiO-67	2591	8.2	3.0	0.5	-	73.7	8.1	[7]
PFC-5	256	-	1.15(5)	0.356(9)	-	-	84	[8]
HOF-BTB	955	-	3.09	0.39	-	-	13.7	[9]
HOF-14	2573	8.09(3)	1.97(1)	0.34(7)	-	28.6	6.3	[10]
ZJU-HOF-8a	863	3.05	2.5	0.50		123[a]	18[a]	[11]
HOF-TCBP	2066	-	-	0.328	-	-	-	[12]
HOF-ZJU-201a	423	2.61	3.16	1.73	-	119	45	[13]
HOF-ZJU-202a	366	1.85	2.53	1.50	-	40	36	[13]
HOF-16	302	-	-	0.339	-	-	-	[14]

a) 0.05/0.95

Table S2. IAST fitting parameter.

	$q_{m,1}$	b_1	n_1	$q_{m,2}$	b_2	n_2	R^2
CH_4	6.5E–2	1.10	5.91	0.39	1.03	1.21	0.999
C_2H_6	4.85	5.1E–3	1.53	1.25	1.82E–2	0.85	0.999
C_3H_8	3.63	0.15	0.78	3.10	0.24	3.20	0.999

Single crystal information

Table S3. X-ray crystallographic data for **YSH-8$_{Ni}$**.

Compound	**YSH-8$_{Ni}$**
Formula	$C_{39}H_{21}N_3Ni_{0.75}O_{12}$
Formula weight	767.62
Temperature, K	298
λ, Å	*tetragonal*
Crystal system	P4/nnc
Space group	24.1698(19)
a, Å	24.1698(19)
b, Å	25.181(4)
c, Å	90
α, °	90
β, °	90
γ, °	90
V, Å^3	14710(3)
Z	8
ρ_{calcd}, g cm^{-3}	0.693
μ, mm^{-1}	0.612
F(000)	3144.0
θ range for data collection, °	5.068 to 136.662
Index ranges	-28 ≤ h ≤ 20, -23 ≤ k ≤ 28, -26 ≤ l ≤ 30
Reflections collected	20460
Independent reflections	6179 [R_{int} = 0.1491, R_{sigma} = 0.1274]
Completeness	99.9
Refinement method	Full-matrix least-squares on F^2
Data/restraints/parameters	6179/6/255
Goodness-of-fit on F^2	1.071
R_1, wR_2 [I>2σ(I)]	0.1581, 0.3622[b]
R_1, wR_2 (all data)	0.1970, 0.3923[b]
Largest peak & hole, eÅ^{-3}	2.34 and -0.51
CCDC number	2324254

[a] $R = \Sigma||Fo| - |Fc||/\Sigma|Fo|$; $wR(F^2) = [\Sigma w(Fo^2 - Fc^2)^2/\Sigma w(Fo^2)^2]^{1/2}$ where $w = 1/[\sigma^2(Fo^2) + (0.1000P)^2]$, $P = (Fo^2 + 2Fc^2)/3$.

[b] $R = \Sigma||Fo| - |Fc||/\Sigma|Fo|$; $wR(F^2) = [\Sigma w(Fo^2 - Fc^2)^2/\Sigma w(Fo^2)^2]^{1/2}$ where $w = 1/[\sigma^2(Fo^2) + (0.2000P)^2]$, $P = (Fo^2 + 2Fc^2)/3$.

Table S4. Hydrogen bonds for **YSH-8$_{Ni}$**.

D-H···A	*d*(H···A) [Å]	*d*(D···A) [Å]	∠(DHA)
O(11)-H(11)···O(31)	1.81	2.621(8)	169.7
O(11)-H(11)···O(12)	1.81	2.614(8)	167.7

Table S5. X-ray crystallographic data for **YSH-8$_{Zn}$**.

Compound	**YSH-8$_{Zn}$**
Formula	$Zn_2C_{104}H_{56}N_8O_{34}$
Formula weight	2092.34
Temperature, K	173(2)
λ, Å	0.71073
Crystal system	*Tetragonal*
Space group	$P\bar{4}2c$
a, Å	23.881(5)
b, Å	23.881(5)
c, Å	16.664(5)
α, °	90
β, °	90
γ, °	90
V, Å^3	9503(5)
Z	2
ρ_{calcd}, g cm^{-3}	0.733
μ, mm^{-1}	0.299
F(000)	2144
θ range for data collection, °	2.961 to 24.296
Index ranges	$-27 \le h \le 27$, $-27 \le k \le 27$, $-18 \le l \le 19$
Reflections collected	50510
Independent reflections	7724 [*R*(int) = 0.1267]
Completeness	99.5 (to theta = 24.296°)
Refinement method	Full-matrix least-squares on F^2
Data/restraints/parameters	7724 / 369 / 297
Goodness-of-fit on F^2	1.680
R_1, wR_2 [$I>2\sigma(I)$]	0.1076, 0.2742[b]
R_1, wR_2 (all data)	0.1537, 0.2975[b]
Largest peak & hole, eÅ^{-3}	0.761 and -0.664
CCDC number	2159884

[a] $R = \Sigma||Fo| - |Fc||/\Sigma|Fo|$; $wR(F^2) = [\Sigma w(Fo^2 - Fc^2)^2/\Sigma w(Fo^2)^2]^{1/2}$ where $w = 1/[\sigma^2(Fo^2) + (0.1000P)^2]$, $P = (Fo^2 + 2Fc^2)/3$.

[b] $R = \Sigma||Fo| - |Fc||/\Sigma|Fo|$; $wR(F^2) = [\Sigma w(Fo^2 - Fc^2)^2/\Sigma w(Fo^2)^2]^{1/2}$ where $w = 1/[\sigma^2(Fo^2) + (0.2000P)^2]$, $P = (Fo^2 + 2Fc^2)/3$.

Table S6. Hydrogen bonds for **YSH-8$_{Zn}$**.

D-H···A	*d*(H···A) [Å]	*d*(D···A) [Å]	∠(DHA)
O(15)-H(15)···O(18)$^{\#1}$	1.77	2.551(11)	153.2
O(19)-H(19)···O(16)$^{\#2}$	1.79	2.577(10)	156.3
O(34)-H(34)···O(37)$^{\#3}$	1.76	2.588(15)	166.3
O(36)-H(36)···O(33)$^{\#4}$	1.84	2.650(14)	162.4

Symmetry transformations used to generate equivalent atoms:

$^{\#1}$11 1-Y, 1-X, -1/2+Z; $^{\#2}$12 1-Y, 1-X, 1/2+Z; #3 +Y, +X, -1/2+Z; #4+Y, +X, 1/2+Z

Table S7. X-ray crystallographic data for **YSH-8$_{Zn/Hx}$**.

Compound	YSH-8$_{Zn/Hx}$
Formula	$Zn_2C_{104}H_{56}N_8O_{33}$
Formula weight	2076.30
Temperature, K	173(2)
λ, Å	0.70000
Crystal system	*Tetragonal*
Space group	*P*4/*nnc*
a, Å	23.745(5)
b, Å	23.745(5)
c, Å	16.703(3)
α, °	90
β, °	90
γ, °	90
V, Å^3	9418(4)
Z	2
ρ_{calcd}, g cm^{-3}	0.732
μ, mm^{-1}	0.289
F(000)	2120
θ range for data collection, °	1.194 to 32.652
Index ranges	$-28\le h\le 30$, $-29\le k\le 26$, $-22\le l\le 22$
Reflections collected	47460
Independent reflections	4608 [*R*(int) = 0.0884]
Completeness	99.3% (to theta = 24.835°)
Refinement method	Full-matrix least-squares on F^2
Data/restraints/parameters	4608 / 0 / 170
Goodness-of-fit on F^2	0.983
R_1, wR_2 [$I>2\sigma(I)$]	0.0583, 0.1962[a]
R_1, wR_2 (all data)	0.0916, 0.2090[a]
Largest peak & hole, eÅ^{-3}	1.338 and –0.372
CCDC number	2159880

[a] $R = \Sigma||Fo| - |Fc||/\Sigma|Fo|$; $wR(F^2) = [\Sigma w(Fo^2 - Fc^2)^2/\Sigma w(Fo^2)^2]^{1/2}$ where $w = 1/[\sigma^2(Fo^2) + (0.1287P)^2]$, $P = (Fo^2 + 2Fc^2)/3$.

Table S8. Hydrogen bonds for **YSH-8$_{Zn/Hx}$**.

D–H···A	*d*(H···A) [Å]	*d*(D···A) [Å]	∠(DHA)
O(2) –H(2)···O(3)$^{\#1}$	1.85	2.589(3)	145.5
O(4) –H(4)···O(1)$^{\#2}$	1.86	2.621(3)	150.2

Symmetry transformations used to generate equivalent atoms:

References

1. Zhang, X.-X.; Guo, X.-Z.; Chen, S.-S.; Kang, H.-W.; Zhao, Y.; Gao, J.-X.; Xiong, G.-Z.; Hou, L., A stable microporous framework with multiple accessible adsorption sites for high capacity adsorption and efficient separation of light hydrocarbons. *Chem. Eng. J.* **2023,** *466*, 143170.

2. Zhou, J.; Ke, T.; Steinke, F.; Stock, N.; Zhang, Z.; Bao, Z.; He, X.; Ren, Q.; Yang, Q., Tunable Confined Aliphatic Pore Environment in Robust Metal–Organic Frameworks for Efficient Separation of Gases with a Similar Structure. *J. Am. Chem. Soc.* **2022,** *144* (31), 14322-14329.

3. Wang, X.; Zhang, X.; Zhang, K.; Wang, X.; Wang, Y.; Fan, W.; Dai, F., Amino-functionalized Cu-MOF for efficient purification of methane from light hydrocarbons and excellent catalytic performance. *Inorganic Chemistry Frontiers* **2019,** *6* (5), 1152-1157.

4. Zhang, Y.; Yang, L.; Wang, L.; Duttwyler, S.; Xing, H., A Microporous Metal-Organic Framework Supramolecularly Assembled from a CuII Dodecaborate Cluster Complex for Selective Gas Separation. *Angew. Chem. Int. Ed.* **2019,** *58* (24), 8145-8150.

5. Fan, W.; Wang, X.; Xu, B.; Wang, Y.; Liu, D.; Zhang, M.; Shang, Y.; Dai, F.; Zhang, L.; Sun, D., Amino-functionalized MOFs with high physicochemical stability for efficient gas storage/separation, dye adsorption and catalytic performance. *J. Mater. Chem. A* **2018,** *6* (47), 24486-24495.

6. Gu, J.; Sun, X.; Kan, L.; Qiao, J.; Li, G.; Liu, Y., Structural Regulation and Light Hydrocarbon Adsorption/Separation of Three Zirconium–Organic Frameworks Based on Different V-Shaped Ligands. *ACS Appl. Mater. Interfaces* **2021,** *13* (35), 41680-41687.

7. Lin, R.-G.; Li, L.; Lin, R.-B.; Arman, H.; Chen, B., Separation of C2/C1 hydrocarbons through a gate-opening effect in a microporous metal–organic framework. *CrystEngComm* **2017,** *19* (45), 6896-6901.

8. Yin, Q.; Lü, J.; Li, H.-F.; Liu, T.-F.; Cao, R., Robust Microporous Porphyrin-Based Hydrogen-Bonded Organic Framework for Highly Selective Separation of C2 Hydrocarbons versus Methane. *Crystal Growth & Design* **2019,** *19* (7), 4157-4161.

9. Yoon, T.-U.; Baek, S. B.; Kim, D.; Kim, E.-J.; Lee, W.-G.; Singh, B. K.; Lah, M. S.; Bae, Y.-S.; Kim, K. S., Efficient separation of C2 hydrocarbons in a permanently porous hydrogen-bonded organic framework. *Chem. Commun.* **2018,** *54* (67), 9360-9363.

10. Wang, B.; Lv, X.-L.; Lv, J.; Ma, L.; Lin, R.-B.; Cui, H.; Zhang, J.; Zhang, Z.; Xiang, S.; Chen, B., A novel mesoporous hydrogen-bonded organic framework with high porosity and stability. *Chem. Commun.* **2020,** *56* (1), 66-69.

11. Jiang, C.; Wang, J.-X.; Liu, D.; Wu, E.; Gu, X.-W.; Zhang, X.; Li, B.; Chen, B.; Qian, G., Supramolecular Entanglement in a Hydrogen-Bonded Organic Framework Enables Flexible-Robust Porosity for Highly Efficient Purification of Natural Gas. *Angew. Chem. Int. Ed.* **2024,** *63* (26), e202404734.

12. Hu, F.; Liu, C.; Wu, M.; Pang, J.; Jiang, F.; Yuan, D.; Hong, M., An Ultrastable and Easily Regenerated Hydrogen-Bonded Organic Molecular Framework with Permanent Porosity. *Angew. Chem. Int. Ed.* **2017,** *56* (8), 2101-2104.

13. Liu, Y.; Xu, Q.; Chen, L.; Song, C.; Yang, Q.; Zhang, Z.; Lu, D.; Yang, Y.; Ren, Q.; Bao, Z., Hydrogen-bonded metal-nucleobase frameworks for highly selective capture of ethane/propane from methane and methane/nitrogen separation. *Nano Research* **2022,** *15* (8), 7695-7702.

14. Cai, Y.; Chen, H.; Liu, P.; Chen, J.; Xu, H.; Alshahrani, T.; Li, L.; Chen, B.; Gao, J., Robust microporous hydrogen−bonded organic framework for highly selective purification of methane from natural gas. *Microporous Mesoporous Mater.* **2023,** *352*, 112495.